

# Superconducting Gap and Strong In-Plane Anisotropy in Untwinned $\text{YBa}_2\text{Cu}_3\text{O}_{7-\delta}$

D. H. Lu, D. L. Feng, N. P. Armitage, K. M. Shen, A. Damascelli, C. Kim, F. Ronning, and Z.-X. Shen  
*Department of Physics, Applied Physics and Stanford Synchrotron Radiation Laboratory,  
Stanford University, Stanford, CA 94305, USA*

D. A. Bonn, R. Liang, and W. N. Hardy  
*Department of Physics and Astronomy, University of British Columbia, Vancouver, BC V6T 1Z1, Canada*

A. I. Rykov and S. Tajima  
*Superconductivity Research Laboratory, International Superconductivity Technology Center,  
1-10-13, Shinonome, Koto-ku, Tokyo 135-0062, Japan*  
(Received 23 January 2001)

With significantly improved sample quality and instrumental resolution, we clearly identify in the  $(\pi, 0)$  ARPES spectra from  $\text{YBa}_2\text{Cu}_3\text{O}_{6.993}$ , in the superconducting state, the long-sought ‘peak-dip-hump’ structure. This advance allows us to investigate the large  $a$ - $b$  anisotropy of the in-plane electronic structure including, in particular, a 50% difference in the magnitude of the superconducting gap that scales with the energy position of the hump feature. This anisotropy, likely induced by the presence of the CuO chains, raises serious questions about attempts to quantitatively explain the  $\text{YBa}_2\text{Cu}_3\text{O}_{7-\delta}$  data from various experiments using models based on a perfectly square lattice.

PACS numbers: 74.25.Jb, 74.72.Bk, 79.60.Bm

High-temperature superconductivity (HTSC) is intimately related to the  $\text{CuO}_2$  plane, which is the only common structural feature in all cuprates. This fact has led most of the proposed microscopic theories to assume a  $\text{CuO}_2$  square planar structure. However, for the practical reason of sample quality, some of the most important and defining experiments have been performed on  $\text{YBa}_2\text{Cu}_3\text{O}_{7-\delta}$  (Y123), which does not have a square lattice, but rather an orthorhombic structure ( $b/a \approx 1.015$ ), caused by the presence of a CuO chain layer [1]. This orthorhombicity, according to LDA calculation [2], should result in significant anisotropy in the *in-plane* electronic structure (this term will be used throughout this paper to refer to the electronic states associated with the  $\text{CuO}_2$  plane), making it problematic to compare theories based on a square lattice with experimental data from Y123. Therefore, it is crucial to quantify the effect of orthorhombicity, if any, on the in-plane electronic structure in Y123. The problem is that angle-resolved photoemission spectroscopy (ARPES), being a uniquely powerful tool for this important task, has, until now, not been particularly effective for the study of Y123 [3]. The important ‘peak-dip-hump’ structure, which is seen routinely in  $\text{Bi}_2\text{Sr}_2\text{CaCu}_2\text{O}_{8+\delta}$  (Bi2212) [4] has never been observed in Y123. This absence, together with the presence of a surface state [5], raises questions about ARPES data from Y123, and the universality of the superconducting peak in the cuprates.

This paper reports a breakthrough in this important issue, made possible by significantly improved sample quality and instrumental resolution. By isolating a surface state peak near the Fermi energy ( $E_F$ ), we can clearly resolve a ‘peak-dip-hump’ structure in the ARPES spectra

around  $(\pi, 0)$  in Y123 that resembles the superconducting peak observed in Bi2212 [4]. More significantly, we find a strong  $a$ - $b$  asymmetry of the in-plane electronic structure, such as the superconducting gap magnitude, which differs by about 50%. We argue that such a strong in-plane  $a$ - $b$  anisotropy should be taken into account when interpreting experiments performed on Y123.

ARPES experiments were carried out at beamline 5-4 at SSRL, which is equipped with a normal-incidence monochromator and a SCIENTA SES-200 analyzer. Untwinned  $\text{YBa}_2\text{Cu}_3\text{O}_{6.993}$  single crystals (overdoped,  $T_c = 89$  K) with superior chemical purity (99.99 – 99.995%) and crystallinity (FWHM =  $0.007^\circ$  in the X-ray rocking curve) were grown by the self-flux method in  $\text{BaZrO}_3$  crucibles [6]. Single crystals were cleaved *in-situ* at 10 K with a base pressure better than  $5 \times 10^{-11}$  torr. ARPES spectra were recorded at a photon energy of 28 eV with an energy resolution of 10 meV and an angular resolution of  $0.3^\circ$ , corresponding to a momentum resolution of 1.5% of the Brillouin zone (BZ). Low energy electron diffraction (LEED) patterns were routinely acquired at the end of experiments to check the quality of the cleaved surfaces and to confirm the sample orientation.

Fig. 1 presents the energy distribution curves (EDCs) along high symmetry directions in the BZ. Data were taken at 10 K under two distinct sample orientations with respect to the polarization of the incoming radiation (insets), which are referred to as O4 and O2, following the existing notation [5]. In order to show the dispersion clearly, in particular for the broad and weak features, the intensity plots of the second derivatives of the EDCs are displayed in Fig. 2a-2f. Four features can be clearly identified, two of which appear at X as sharp peaks close to

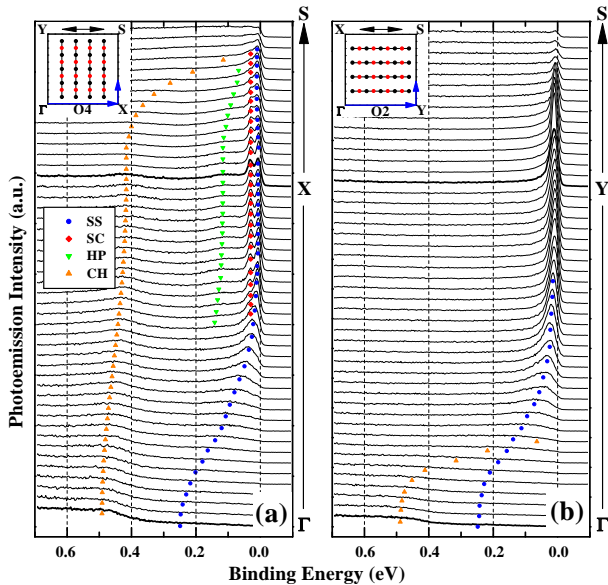


FIG. 1. (color) ARPES spectra taken at 10 K on untwinned  $\text{YBa}_2\text{Cu}_3\text{O}_{6.993}$  along (a)  $\Gamma$ -X-S and (b)  $\Gamma$ -Y-S. The insets depict the sample orientations (black and red circles represent the CuO chains) with respect to the linear photon polarization (black arrows). Four features in the spectra, labeled as SS, SC, HP, and CH, correspond to surface state, superconducting peak, hump, and chain state, respectively (see text).

$E_F$ , along with two broad features at higher binding energy (BE). As we will justify in the following paragraphs, we assign them, from the lower to higher BE, as surface state, superconducting peak, hump, and chain state. Fig. 2g summarizes all of the band dispersions.

The most pronounced feature in Fig. 1 is a narrow, intense peak just below  $E_F$  at both X and Y, whose high sensitivity to surface degradation at elevated temperatures indicates its surface state character. The precise origin of this surface state is, however, not well understood at present. One possibility could be the surface termination effect. An earlier scanning tunneling microscopy (STM) study [7] demonstrated that Y123 cleaves between the CuO chain and BaO layers, resulting in both CuO chain-terminated and BaO-terminated areas on the cleaved surface. The scenario of a chain-related surface state is favored by a previous ARPES study [5], and seems to be consistent with more recent STM data [8]. However, this assignment is difficult to reconcile with the two-dimensional dispersion of this feature along  $\Gamma$ -X and  $\Gamma$ -Y, as seen in the current data. For this paper, as we will focus on the bulk electronic structure, we leave it as an open question.

For the broad feature located well below  $E_F$  at X, instead of a bonding  $\sigma$  state as suggested in Ref. [5], we reassign it to a chain derived state. This assignment is concluded from the quasi one-dimensional (1D) character of this feature, *i.e.*, the dispersion is strong along the chain direction ( $\Gamma$ -Y and X-S) and weak in the perpen-

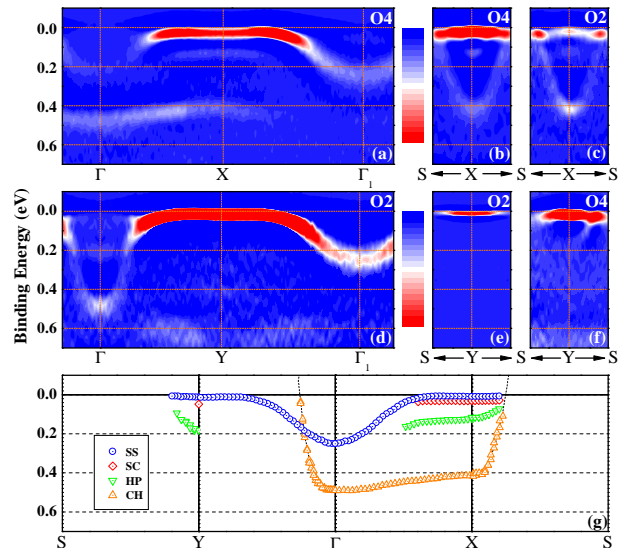


FIG. 2. (color) (a)-(f) Second derivatives of the ARPES spectra along high symmetry lines with different sample orientations. The red-white-blue color scale is chosen to emphasize the broad features that are difficult to resolve in the EDCs. Bottom panel (g) summarizes all of the band dispersions.

dicular direction ( $\Gamma$ -X). Further support comes from the fact that the two crossings along  $\Gamma$ -Y and X-S agree very well with the 1D chain Fermi surface (FS) determined by a full FS mapping. The dispersion of this chain state and the related chain FS are consistent with the LDA band structure [2]. It is also interesting to note that this feature looks rather similar to the chain state observed in  $\text{PrBa}_2\text{Cu}_3\text{O}_7$  [9] and that the dispersion along the chain direction qualitatively agrees with the holon band predicted by the  $t$ - $J$  model calculation at quarter filling [10]. However, we were not able to identify in the current data a spinon band, which may possibly be masked by the hump around 0.12 eV in Y123.

Now let us focus on the superconducting peak and the hump that are clearly evident in Fig. 1a. For better illustration, the EDC at X is replotted in Fig. 3a with fitting curves. In the fitting procedure, an integration background that smoothly merges into the high-energy hump is subtracted to extract the double peak feature, which is then fitted with a simple spectral function: a product of a Fermi function and two Lorentzians, convolved with a gaussian instrumental resolution function. After subtracting the surface state peak, the rest of the spectrum looks strikingly similar to the well-known ‘peak-dip-hump’ structure observed in the ARPES spectra of Bi2212 at  $(\pi, 0)$  below  $T_c$  (Fig. 3b), indicating that the second peak may be a superconducting peak.

More direct evidence of the superconducting nature of this peak comes from its temperature dependence (Fig. 4a). Due to the unstable nature of the Y123 surface at high temperatures, great caution has been taken in cycling the temperature. A LEED pattern taken after

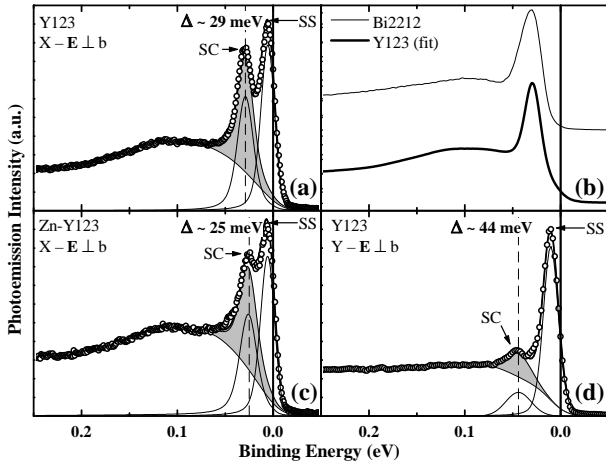


FIG. 3. (a) EDC at X reproduced from Fig. 1a together with fitting curves. Panel (b) compares the fitting curve (after subtracting the surface state peak) with the EDC from overdoped Bi2212 ( $T_c = 84$  K) at  $(\pi, 0)$ . (c) EDC at X from Zn-doped Y123 with fitting curves. (d) EDC at Y from Y123 with fitting curves. All data shown were taken at 10 K. Shaded area represents weight of the superconducting peak.

the measurements (Fig. 4b) shows no visible difference from that of a freshly cleaved surface, indicating a well-ordered surface, although some minor aging effects can be detected. Following the same fitting procedure (with both peak positions fixed), we extract the superconducting peak and plot in Fig. 4c the normalized superconducting peak ratio (SPR), which is defined after Ref. [11] as the ratio between the extracted peak intensity and the total spectral weight (excluding the surface state peak) integrated over  $[0.3 \text{ eV}, -0.1 \text{ eV}]$ . Despite the scatter in the data and the large error bars, the general trend suggests that the appearance of this peak is related to the superconducting transition.

Furthermore, the remarkable resemblance of the spectra in Fig. 3b implies that this ‘peak-dip-hump’ structure at X is a  $\text{CuO}_2$  plane derived feature since the  $\text{CuO}$  chain is absent in Bi2212. This argument is further supported by data taken on Zn-doped ( $\sim 2\%$ ) Y123 with the same oxygen content under identical experimental conditions (Fig. 3c). Compared with the data from Zn-free Y123 (Fig. 3a), the major change is that the superconducting peak shifts to lower BE, *i.e.*, the gap size decreases upon Zn-doping. Since Zn atoms only occupy the Cu sites in the  $\text{CuO}_2$  plane [12], this change in the superconducting peak suggests that it is directly related to the  $\text{CuO}_2$  plane. Due to the weak dispersion of this peak around  $(\pi, 0)$ , we can approximately quantify the superconducting gap using the peak position, giving a gap size of 25 and 29 meV at X for Zn-doped ( $T_c = 79$  K) and Zn-free ( $T_c = 89$  K) Y123, respectively. This indicates that, as expected, the gap magnitude scales with  $T_c$ .

At this point, one may speculate as to why the ‘peak-dip-hump’ feature is absent at Y in Fig. 1b. This is partly

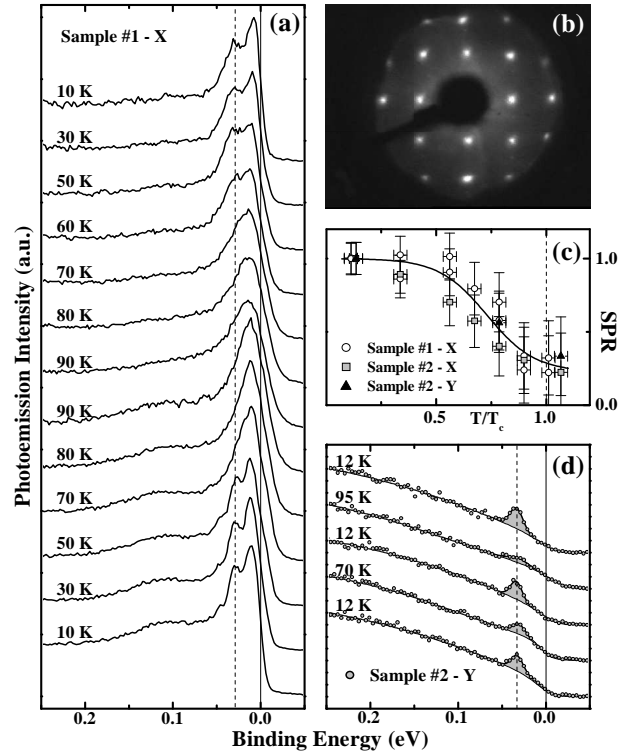


FIG. 4. Temperature dependence of ARPES spectra from Y123 at (a) X-point and (d) Y-point. Data are presented in the order of acquisition starting from the bottom curve of each panel. (b) LEED pattern taken after experiments for panel (a). (c) Normalized SPR (see text) for different samples *vs.* reduced temperature.

due to the presence of the intense surface state peak, which masks the underlying bulk electronic states close to  $E_F$ . In fact, the data taken at Y with the polarization perpendicular to the chain direction (Fig. 3d), where the surface state peak is suppressed, clearly show a second peak at higher BE. In analogy with the assignment of the superconducting peak at X we may reasonably interpret this additional feature as evidence for a superconducting peak at Y. The hump associated with this peak is almost indiscernible in Fig. 3d, but becomes more evident moving away from Y to S as it disperses towards  $E_F$  (Fig. 2f). The temperature dependent measurements on this feature are very difficult due to its weak intensity and the presence of the strong surface state peak. Hence, we deliberately aged the sample by warming it to the point where the surface state peak completely vanishes (Fig. 4d). A small peak on top of a relatively large background exhibits a reproducible temperature dependence expected for a superconducting peak. As a consequence of aging, this peak shifts to lower BE ( $\sim 33$  meV), as compared with Fig. 3d. Since the Y-point is outside the 1D chain FS, the peak and the hump detected at Y should be exclusively related to the  $\text{CuO}_2$  plane.

Having identified all of the features in the low energy excitation spectra, our data provide the first observation

of a ‘peak-dip-hump’ structure near  $(\pi, 0)$  in a system other than Bi2212. This finding partially resolves the longstanding issue regarding the universality of the superconducting peak, which is crucial for a complete understanding of HTSC as it appears to contain information on both pairing and phase coherence [11]. The failure to detect this peak in previous photoemission studies on Y123 was mainly due to the presence of the intense surface state peak and insufficient energy and momentum resolution. However, it is not clear at present whether the absence of this peak in other superconducting cuprates, such as  $\text{Bi}_2\text{Sr}_2\text{CuO}_{6+\delta}$  and  $\text{La}_{2-x}\text{Sr}_x\text{CuO}_4$ , is simply a consequence of lower  $T_c$  [13], *i.e.*, low superfluid density, or is also related to the lack of the  $\text{CuO}_2$  bilayer that exists in both Bi2212 and Y123. Further experiments on other cuprate superconductors, particularly the single-plane Tl- or Hg-based compounds with higher  $T_c$ , are necessary to clarify this issue.

Now let us turn our attention to the strong  $a$ - $b$  anisotropy of the electronic structure as revealed by a direct comparison between Fig. 1a and 1b. For the chain state, the  $a$ - $b$  asymmetry is in accord with the 1D character of the  $\text{CuO}$  chain. More interesting is the  $a$ - $b$  anisotropy associated with the peak and the hump as they are related to the superconductivity in the  $\text{CuO}_2$  plane. The major asymmetry lies in the energy positions of the peak and the hump: 29 ( $\Delta_x$ ) and 120 meV ( $\omega_x$ ) for X, and 44 ( $\Delta_y$ ) and 180 meV ( $\omega_y$ ) for Y. This yields a significant ( $\sim 50\%$ ) difference in the gap magnitude between X and Y, a substantial deviation from the ideal  $d$ -wave pairing state. This  $a$ - $b$  asymmetry of the superconducting gap in Y123 has also been reported by Limonov and co-workers in their Raman scattering study [14], from which a value of 25 and 30 meV can be derived for  $\Delta_x$  and  $\Delta_y$ , respectively. It is also remarkable to see that the gap magnitude scales with the hump positions:  $\Delta_x/\omega_x \approx \Delta_y/\omega_y \approx 0.24$ . The scaling of these two energy scales has also been observed by ARPES in Bi2212 as a function of doping [15,16]. The observation of this scaling behavior in the same material along two different directions imposes strong constraints on theory.

In addition to the asymmetry of the gap magnitude, we also notice that there is a clear difference in the intensities of the peak and the hump between X and Y. According to Ref. [11], this could possibly be a signature of the in-plane anisotropy of the superfluid density. However, the polarization effects due to the presence of the  $\text{CuO}$  chains on the surface layer may complicate the situation, making a quantitative comparison difficult. We note that strong  $a$ - $b$  anisotropy of the penetration depth (*i.e.*, the superfluid density) was also found in microwave and far infrared spectroscopic measurements [17,18], which was interpreted as evidence for the presence of superconductivity in the chain layer. While it is still a controversial issue whether the ground state of the  $\text{CuO}$  chain is superconducting or a charge density wave [19], our data offer

an alternative interpretation: this anisotropy may in fact reside in the  $\text{CuO}_2$  plane itself.

Such a strong  $a$ - $b$  anisotropy is crucial for a comprehensive understanding of the superconducting properties of Y123 and the interpretation of related experiments. It is therefore important to understand the origin of this in-plane anisotropy. One possible explanation could be based on the orthorhombicity of the  $\text{CuO}_2$  plane in Y123. According to the LDA band calculations, the ratio between the hopping integrals along the  $a$  and  $b$  directions scales roughly as  $(b/a)^4$ , which, in turn, yields considerable differences in the calculated electronic structures between  $\Gamma$ -X-S and  $\Gamma$ -Y-S [2] that qualitatively agree with our data. However, no direct conclusion can be drawn for the superconducting state properties. Alternatively, a strong chain-plane coupling may be present. In particular, as recently suggested by Atkinson [20], a nontrivial  $d$ -wave gap structure, which seems to be consistent with our data, exists on the anti-bonding band related FS due to the hybridization with the chain band.

We thank for J. C. Davis, A. L. de Lozanne, H. Eisaki, T. Mizokawa and S. Schuppler for fruitful discussions, T. Tohyama, and S. Maekawa for unpublished results from their calculations. The data presented here were obtained at SSRL, which is operated by the Department of Energy, Office of Basic Energy Sciences. The Stanford work was also supported by ONR Grant N00014-98-1-0195 and NSF grant DMR-9705210.

- 
- [1] J. D. Jorgenson *et al.*, Phys. Rev. B **36**, 3608 (1987).
  - [2] O. K. Andersen, A. I. Liechtenstein, O. Jepsen, and F. Paulsen, J. Phys. Chem. Solids **56**, 1573 (1995).
  - [3] Z.-X. Shen and D. Dessau, Phys. Rep. **253**, 1 (1995).
  - [4] D. S. Dessau *et al.*, Phys. Rev. Lett. **66**, 2160 (1991);
  - [5] M. C. Schabel *et al.*, Phys. Rev. B **57**, 6090 (1998).
  - [6] R. Liang, D. A. Bonn, and W. N. Hardy, Physica C **304**, 105 (1998).
  - [7] H. L. Edwards, J. T. Markert, and A. L. de Lozanne, Phys. Rev. Lett. **69**, 2967 (1992).
  - [8] D. J. Derro, *et al.*, in preparation.
  - [9] T. Mizokawa *et al.*, Phys. Rev. B **60**, 12335 (1999).
  - [10] S. Maekawa, T. Tohyama, and S. Yunoki, Physica C **263**, 61 (1996); T. Tohyama *et al.*, unpublished data.
  - [11] D. L. Feng *et al.*, Science **289**, 277 (2000).
  - [12] G. Xiao *et al.*, Nature **332**, 238 (1988).
  - [13] Even in the Bi2212 system, no superconducting peak has been resolved for samples with  $T_c < 40$  K.
  - [14] M. F. Limonov, A. I. Rykov, S. Tajima, and A. Yamanaka, Phys. Rev. B **61**, 12412 (2000).
  - [15] P. J. White *et al.*, Phys. Rev. B **54**, R15669 (1996).
  - [16] J. C. Campuzano *et al.*, Phys. Rev. Lett. **83**, 3709 (1999).
  - [17] K. Zhang *et al.*, Phys. Rev. Lett. **73**, 2484 (1994).
  - [18] D. N. Basov *et al.*, Phys. Rev. Lett. **74**, 598 (1995).
  - [19] B. Grvin, Y. Berthier, and G. Collin, Phys. Rev. Lett. **85**, 1310 (2000).
  - [20] W. A. Atkinson, Phys. Rev. B **59**, 3377 (1999).